

Title:

Evaluation of Current Sensitivity of Quantum Flux Parametron

Authors and addresses:

Yuki Yamanashi^{1,2}, Takashi Matsushima¹, Naoki Takeuchi^{2,3}, Nobuyuki Yoshikawa^{1,2}, and Thomas Ortlepp^{2,4}

1 Department of Electrical and Computer Engineering, Yokohama National University, 79-5 Tokiwadai, Hodogaya, Yokohama 240-8501, Japan

2 Institute of Advanced Sciences, Yokohama National University, 79-5 Tokiwadai, Hodogaya, Yokohama 240-8501, Japan

3 PRESTO, Japan Science and Technology Agency, 4-1-8 Honcho, Kawaguchi, Saitama 332-0012, Japan

4 CiS Research Institute for Microsensor Systems GmbH, Konrad-Zuse-Straße 14, 99099 Erfurt, Germany

E-mail addresses:

yamanashi-yuki-kr@ynu.ac.jp

Abstract:

Current sensitivity of quantum flux parametron (QFP) was evaluated by measuring gray zone width on the basis of both circuit simulation and measurements for superconducting sensing systems composed of a superconducting sensor array and superconducting read-out and signal processing circuits. Simulation results indicate the narrow gray zone width can be obtained by decreasing inductances comprising the QFP. Moreover, both high-sensitivity and low-power operation of the QFP can be utilized by using optimized circuit parameters and the excitation

current that has long rise time. Gray zone width of approximately $0.5 \mu\text{A}$, which is smaller than that of the Josephson current comparator based on a single flux quantum circuit, was experimentally obtained by using the trapezoidal excitation current that has rise time of $50 \mu\text{s}$. These results indicate the QFP is promising for the read-out circuit in the superconducting sensing systems because of high-sensitivity and low-power operation.

Keywords:

QFP, gray zone, sensor array, Josephson integrated circuit

1. Introduction

A multi-channel superconducting sensor array is an attractive tool for various applications because of its high-sensitivity and special resolution. In the field of magnetoencephalography, a 168-channel SQUID magnetometer has been implemented to measure the distribution of the magnetic field generated by the human brain [1]. However, implementation of a large-scale multi-channel superconducting sensor array is difficult because all superconducting sensor in the low-temperature stages are read-out by room-temperature electronics and it results in drastic increase in the number of cables that connect low-temperature and room-temperature stages. Inflow of thermal noises from the room-temperature environment makes cooling of the sensor array difficult. Furthermore, the performance of the superconducting sensor is limited by the bandwidth of the cables in some applications. Integration of the superconducting sensor array and read-out and signal processing circuits in the same low-temperature stage is one of solutions to overcome the difficulty in implementing large-scale multi-channel superconducting sensor array systems.

A superconducting circuit is thought to be suitable for the read-out circuit for the superconducting sensor array because it can operate in the low temperature environment with ultra-low power consumption. Superconducting sensing systems, where the superconducting sensor array and a superconducting single flux quantum (SFQ) read-out circuit [2, 3] are integrated in the low temperature stage, have been proposed and demonstrated for various applications [4–10]. The number of required cables can be reduced by using signal processing of multiplexing techniques [11–13].

Recently, quantum flux parametron (QFP) [14] has attracted attention as an ultra-low-power superconducting circuit by utilizing an adiabatic driving method [15, 16]. Because the QFP is superior to the SFQ circuit in terms of power consumption and sensitivity, the QFP might be suitable for the read-out and signal processing circuits for the superconducting sensor array.

Sensitivity of the read-out circuit that detects and measures the output signal from the superconducting sensor is the most important information to determine the architecture of the system composed of the superconducting sensor array and QFP read-out circuits.

In this study, we evaluated the current sensitivity of a QFP buffer on the basis of both circuit simulation and experiments. Circuit parameters for improving current sensitivity of the QFP are investigated. We analyzed the relationship between the currents sensitivity and rise time of the excitation current QFP. The relationship between current sensitivity and power consumption of the QFP is discussed.

2. Analysis of QFP current comparator

Figure 1 show the equivalent circuit of the QFP analyzed in this study. The logic state of the QFP is expressed by the direction of the output current I_{out} after circuit excitation. In ideal case where the QFP has symmetric circuit structure and no noise exists, the logic state of the QFP is precisely determined by the direction of the input current. Therefore, the QFP can be used as a current comparator or a 1-bit analog-to-digital modulator that discriminates the direction of the input current [17].

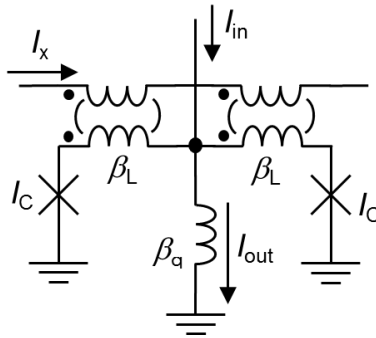


Figure 1. Equivalent circuit of the analyzed QFP. I_C is the critical current of Josephson junctions comprising the QFP. β_L and β_q are inductance values normalized by $\Phi_0/2\pi I_C$, where Φ_0 is the flux quantum in a superconductor.

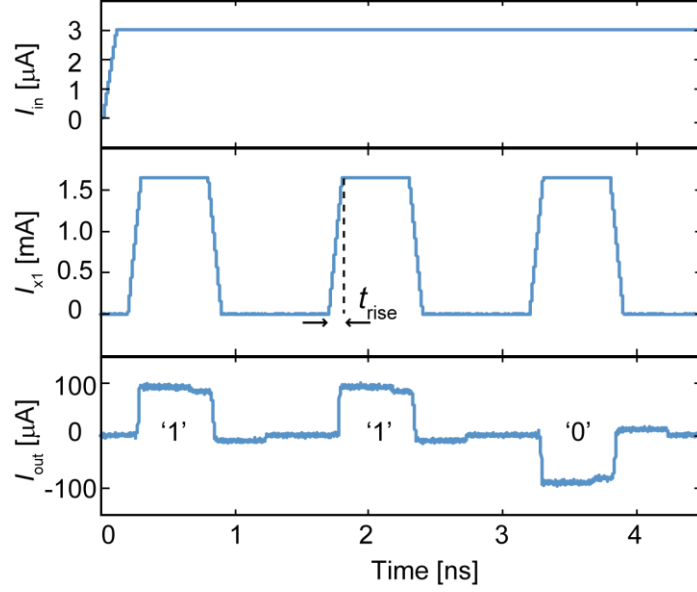


Figure 2. Example of the simulated transient analysis of the QFP. The dc input current of 3 μA is supplied. Rise time of the excitation current (t_{rise}) is 400 ns. Though the input current is positive, the error '0' output is obtained. The critical current of Josephson junctions is 50 μA . Normalized inductances β_L and β_q are 0.2 and 1.6, respectively.

In practical case, the output from the QFP is probabilistic around $I_{\text{in}} = 0$ because of the noises in the circuit. The influence of thermal noise is the main origin of the stochastic characteristics of the QFP operating at 4.2 K [18]. Width of the input current region where the probabilistic output is obtained is called the gray zone. Because the QFP can not discriminate the input current less than gray zone width by a single-shot measurement, current sensitivity of the QFP can be evaluated by measuring the gray zone width.

Figure 2 shows an example of transient analysis of the QFP taking thermal noises at 4.2 K into account by using the JSIM_N [19]. The critical current of the Josephson junction is 50 μA , which is minimum critical current that is insured to be reproducible by the AIST 2.5 kA/cm^2 Nb standard process 2 (STP2) [20, 21]. The McCumber parameter of Josephson junctions β_C is 1, thus, junctions are critically damped. In the simulation, thermal noise source is shunt resistors

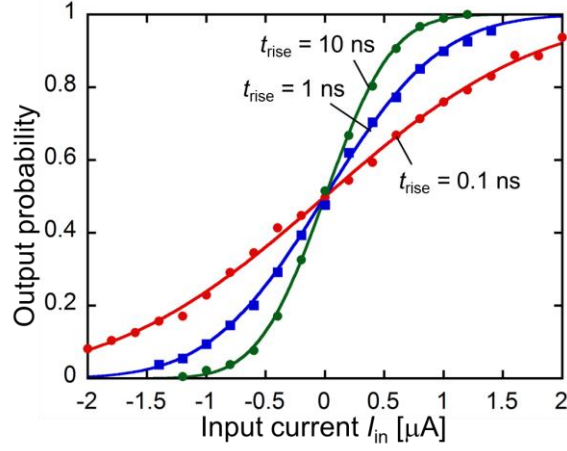


Figure 3. Dependences of simulated output probability of the QFP on the input current for different rise time of the excitation current t_{rise} . β_L is 0.2. Dots are simulation results. Lines are fitting curves.

connected to Josephson junctions in parallel. As shown in figure. 2, some errors are observed caused by thermal noises. We repeated 1000 excitation cycles in the simulation and calculated the dependence of the output probability that the ‘1’ output is obtained on the input current. We systematically simulated the output probability characteristics of the QFP, composed of different inductances, driven by the excitation current that has different rise time.

Figure 3 shows dependences of the output probability of the QFP composed of inductances of $\beta_L = 0.2$ and $\beta_q = 1.6$ on the input current for different rise time of the excitation current. As shown in figure 3, the gray zone of the QFP reduces with increase in rise time of the excitation current I_x . This is because the long decision process reduces the effective bandwidth of thermal noises and therefore reduces its influence [22].

Assuming Gauss distribution of thermal current in the resistors, the output probability of the QFP can be fitted using the error function as

$$P(I_{\text{in}}) = 0.5 + 0.5 \operatorname{erf} \left(\sqrt{\pi} \frac{I_{\text{in}}}{\Delta I} \right), \quad (1)$$

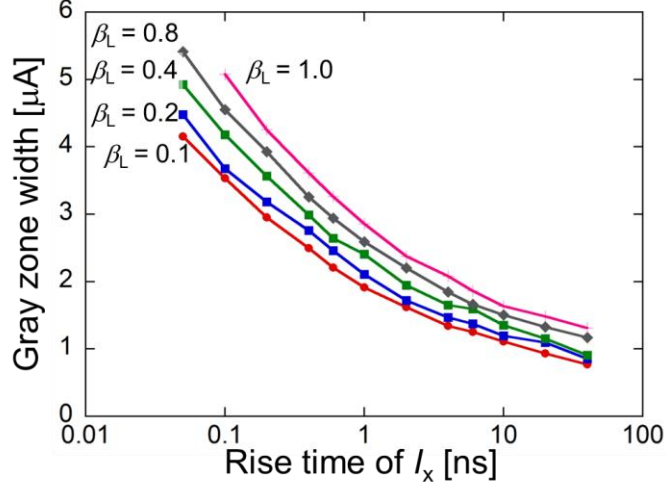


Figure 4. Dependences of gray zone width of the QFP with different β_L on rise time of the excitation current t_{rise} . β_q is 1.6.

where $P(I_{\text{in}})$ is the output probability when the input current I_{in} is supplied and ΔI is the gray zone width.

Figure 4 shows the simulated dependences of gray zone width of the QFP composed of different β_L on rise time of the excitation current t_{rise} . β_L of 0.1 corresponds to the inductance of 0.62 pH, which is almost the minimum inductance value that can be implemented using the AIST-ADP2 [20, 21]. The circuit simulation results indicate the narrow gray zone width of the QFP can be obtained by using small β_L and long t_{rise} . Therefore, trade-off between current sensitivity and decision time of the QFP is confirmed like the Josephson current comparator based on the SFQ circuit [22].

We analyzed the relationship between gray zone width and energy consumption of the QFP. Energy consumption per bit was calculated by integrating the product of the current and voltage in the excitation current line in one excitation cycle using JSIM_N. Figure 5 summarize the relationship between energy consumption per bit operation and gray zone width of the QFP. Bit energy of the non-adiabatic superconducting circuit is approximately $\Phi_0 I_C \sim 10^{-19}$ J/bit.

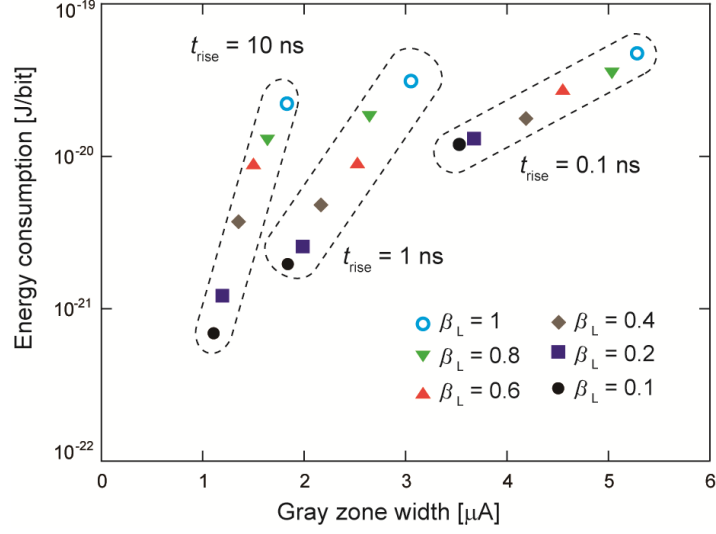


Figure 5 Relationship between energy consumption per bit operation and gray zone width of the QFP.

Therefore, less than 1% of $\Phi_0 I_C$ bit energy operation is achieved when the QFP composed of $\beta_L = 0.1$ is driven by the excitation current with rise time of 10 ns. Moreover, both small gray zone and small energy consumption of the QFP can be achieved by decreasing inductances in the QFP and increasing decision time.

3. Experimental and Discussion

We designed a test circuit to measure gray zone width of the QFP using the STP2. β_L and β_q of the designed QFP are 0.221 and of 1.18, respectively. Inductances were extracted by the circuit layout using the InductEX [23]. Figure 6 shows the microphotograph of the test circuit. The measured QFP is placed in the first stage of the QFP buffer chain. 5 stages of AQFP buffers are inserted after the QFP under test. The test chip was cooled and measured at 4.2 K in a liquid helium bath. The input current was injected to the first stage from a current source in the room-temperature environment. The output is read-out by the adequately biased dc-SQUID. We employed the 3-phase excitation method [15] to drive the AQFP buffer chain.

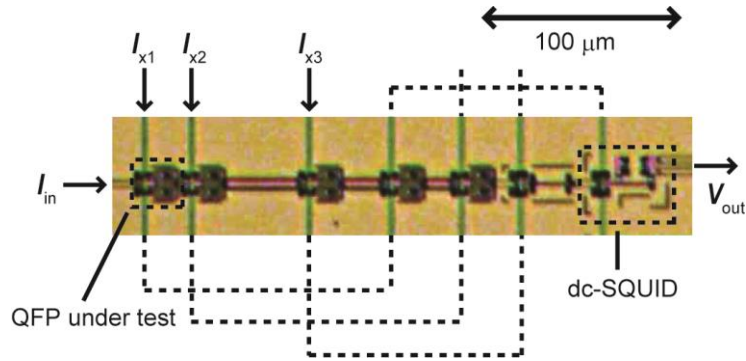


Figure 6 Microphotograph of the QFP buffer chain. Gray zone width of the first stage QFP is measured. All QFPs are composed of Josephson junctions with the critical current of 50 μA . The QFP under test has $\beta_L = 0.221$ and $\beta_q = 1.18$.

Figure 7 shows the measured waveform when the QFP is driven by the excitation current with rise time of 400 ns. Arbitrary function generators were used to generate trapezoidal three-phase excitation currents. The output probability was automatically measured by measuring the output voltage from dc-SQUID magnetically connected to the sixth stage QFP

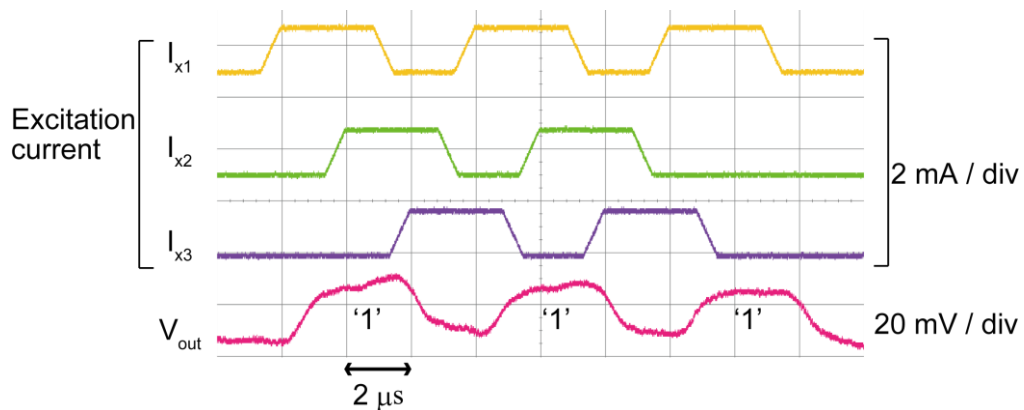


Figure 7 Example of the measured waveform when $I_{in} = 1 \mu\text{A}$ was input. The output voltage was amplified by a low-noise differential amplifier by 100. The output probability was measured by repeating 1000 excitation cycles. '1' output is obtained every clock cycle in this output pattern.

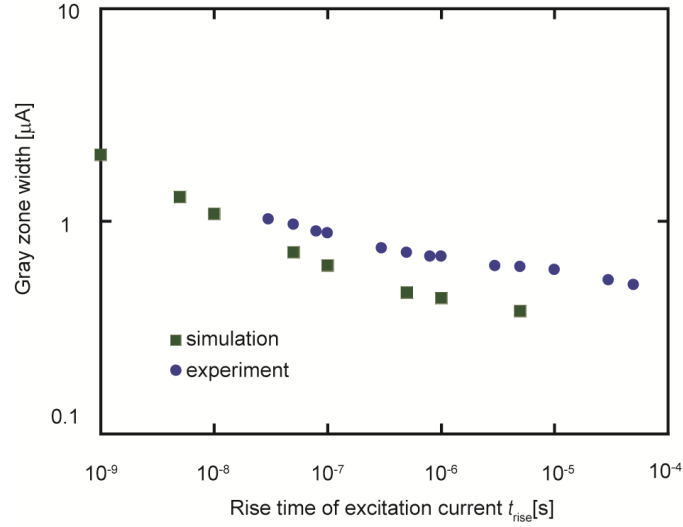


Figure 8 Comparison of measured and simulated dependences of gray zone width on t_{rise} .

buffer.

Figure 8 shows simulated and measured dependences of gray zone width on t_{rise} . Experimentally obtained gray zone width of the QFP was approximately 0.5 μA when t_{rise} of 50 μs was used. The experimental results indicate current sensitivity of the QFP is better than Josephson current comparator [24] and the QFP is suitable for the read-out circuit for the superconducting sensor array in terms of current sensitivity.

The measured gray zone characteristic of the QFP shows the same tendency as the simulated result. However, discrepancy between measured and simulated gray zone width increases with increase in rise time of the excitation current. This might be caused by an influence of $1/f$ noise, which is caused by the motion of trapped charges in a Josephson junction and critical in superconducting quantum bit (qubit) applications [25–27]. Because the typical operating frequency of SFQ circuits, which is determined by switching speed of Josephson junctions, is extremely higher than the frequency range where $1/f$ noise is dominant in superconducting circuits, the influence of the $1/f$ noise has been neglected in simulation of SFQ circuits [22, 24]. However, the influence of $1/f$ noise is thought to be considered when the excitation current with

long rise time is used to drive the QFP. More detailed studies are required to clarify the influences of $1/f$ noise on the QFP operation.

4. Conclusion

We investigated current sensitivity of the QFP buffer by evaluating the gray zone width. Current sensitivity of the QFP buffers depends on inductances comprising the QFP and the decision time of the logic state. Simulation results show the QFP composed of small inductances driven by the excitation current with long rise time has both low-power operation and high-sensitivity. The measured gray zone characteristics show good agreement with simulated result. Current sensitivity of the QFP higher than the Josephson current comparator was experimentally demonstrated.

Acknowledgement

This work was supported by JSPS KAKENHI Grant Number JP26220904 and conducted under the auspices of the MEXT Program for Promoting the Reform of National Universities. The circuits were fabricated in the clean room for analog-digital superconductivity (CRAVITY) of AIST with the standard process 2 (STP2). The AIST-STP2 is based on the Nb circuit fabrication process developed in ISTECH.

References

- [1] Rombetto S, Granata S, Vettoliere A and Russo M 2014 Multichannel System Based on a High Sensitivity Superconductive Sensor for Magnetoencephalography *Sensors* **2014** 12114–12126

- [2] Likharev K K and Semenov V K 1991 RSFQ logic/memory family: a new Josephson-junction technology for sub-terahertz-clock-digital systems *IEEE Trans. Appl. Supercond.* **1** 3–28
- [3] Nakajima K, Mizusawa H, Sugahara H and Sawada Y 1991 Phase Mode Josephson Computer System *IEEE Trans. Appl. Supercond.* **1** 29–36
- [4] Reich T, Ortlepp T, Uhlmann F H 2005 Digital SQUID Sensor Based on SFQ Technique *IEEE Trans. Appl. Supercond.* **15** 304–307
- [5] Terai H, Miki S and Wang Z 2009 Readout Electronics Using Single-Flux-Quantum Circuit Technology for Superconducting Single-Photon Detector Array *IEEE Trans. Appl. Supercond.* **19** 350–353
- [6] Myoren H, Kimimoto Y, Terui K and Taino T 2011 Design of Digital DROS With SFQ Up/Down Counter for Wide Dynamic Operation Range *IEEE Trans. Appl. Supercond.* **21** 387–390
- [7] Ortlepp T, Hofherr M, Fritzsche L, Engert S, Ilin K, Rall D, Toepfer H, Meyer H G and Siegel M 2011 Demonstration of digital readout circuit for superconducting nanowire single photon detector *Opt. Express* **19** 18593-18601
- [8] Miki S, Terai H, Yamashita T, Makise K, Fujiwara M, Sasaki M and Wang Z 2011 Superconducting single photon detectors integrated with single flux quantum readout circuits in a cryocooler *Appl. Phys. Lett.* **99** 111108
- [9] Miyajima S, Kusumoto T, Ito K, Akita Y, Yagi I, Yoshioka N, Ishida T, Miki S, Wang Z and Fujimaki A 2013 High-Throughput RSFQ Signal Processor for a Neutron Diffraction System With Multiple MgB₂ Detectors *IEEE Trans. Appl. Supercond.* **23** 1800505
- [10] Sano K, Takahashi Y, Yamanashi Y, Yoshikawa N, Zen N and Ohkubo M 2015 Demonstration of single-flux-quantum readout circuits for time-of-flight mass spectrometry systems using superconducting strip ion detectors *Supercond. Sci. Technol.* **28** 074003

- [11] Hofherr M, Wetzstein O, Engert S, Ortlepp T, Berg B, Ilin K, Henrich D, Stolz R, Toepfer H, Meyer H G and Siegel M 2012 Orthogonal sequencing multiplexer for superconducting nanowire single-photon detectors with RSFQ electronics readout circuit *Opt. Express* **20** 28683-28697
- [12] Aoki K, Yamanashi Y and Yoshikawa N 2013 Multiplexing Techniques of Single Flux Quantum Circuit Based Readout Circuit for a Multi-Channel Sensing System *IEEE Trans. Appl. Supercond.* **23** 2500204
- [13] Sahu A, Filippov T, Radparvar M, Kirichenko D and Guputa D 2017 *IEEE Trans. Appl. Supercond.* **17** 2500106
- [14] Hosoya M, Hioe W, Casas J, Kamikawai R, Harada Y, Wada Y, Nakane H, Suda R and Goto E 1991 Quantum flux parametron: a single quantum flux device for Josephson supercomputer *IEEE Trans. Appl. Supercond.* **1** 77–89
- [15] Takeuchi N, Ozawa D, Yamanashi Y and Yoshikawa N 2013 An adiabatic quantum flux parametron as an ultra-low power logic device *Supercond. Sci. Technol.* **26** 35010
- [16] Takeuchi N, Yamanashi Y and Yoshikawa N 2013 Measurement of 10 zJ energy dissipation of adiabatic quantum-flux parametron logic using a superconducting resonator *Appl. Phys. Lett.* **102** 052602
- [17] Ko H L, Lee G S and Ruby R C 1993 A SINGLE QFP TIMING DISCRIMINATOR *IEEE Trans. Appl. Supercond.* **3** 2756–2759
- [18] Takeuchi N, Yamanashi Y and Yoshikawa N 2013 Simulation of sub- $k_B T$ bit-energy operation of adiabatic quantum-flux-parametron logic with low bit-error-rate *Appl. Phys. Lett.* **103** 062602
- [19] Satchell J 1997 Stochastic Simulation of SFQ Logic *IEEE Trans. Appl. Supercond.* **7** 3315–3318
- [20] Nagasawa S, Hashimoto Y, Numata H and Tahara S 1995 A 380 ps, 9.5 mW Josephson

4-Kbit RAM operated at a high bit yield *IEEE Trans. Appl. Supercond.* **5** 2447–2452

[21] Hidaka M, Nagasawa S, Satoh T, Hinode K and Kitagawa Y 2006 Current status and future prospect of the Nb-based fabrication process for single flux quantum circuits *Supercond. Sci. Technol.* **19** S138–S145

[22] Ortlepp T, Volkmann M H and Yamanashi Y 2014 Memory effect in balanced Josephson comparators *Physica C* **500** 20–24

[23] Fourie C J, Wetzstein O, Ortlepp T and Kunert J 2011 Three-dimensional multi-terminal superconductive integrated circuit inductance extraction *Supercond. Sci. Technol.* **24** 125015

[24] Ortlepp T, Miyajima S, Toepfer H and Fujimaki A 2012 Josephson comparator with modified dynamic behavior for improved sensitivity *J. Appl. Phys.* **111** 123901

[25] Wellstood F C, Urbina C and Clarke J 2004 Flicker ($1/f$) noise in the critical current of Josephson junctions at 0.09–4.2 K *Appl. Phys. Lett.* **85**, 5296

[26] Martinis J M, Nam S, Aumentado J, Lang K M and Urbina C 2003 Decoherence of a superconducting qubit due to bias noise *Phys. Rev. B* **67** 094510

[27] Mück M, Korn M, Mugford C G, Kycia J B and Clarke J 2005 Measurements of $1/f$ noise in Josephson junctions at zero voltage: Implications for decoherence in superconducting quantum bits *Appl. Phys. Lett.* **86** 012510